THE JOURNAL OF BIOLOGICAL CHEMISTRY
Vol. 277, No. 8, Issue of February 22, pp. 6273–6279, 2002
Printed in U.S.A.

Cholesterol Is an Important Factor Affecting the Membrane Insertion of β-Amyloid Peptide (Aβ1–40), Which May Potentially Inhibit the Fibril Formation*

Received for publication, May 8, 2001, and in revised form, December 2, 2001
Published, JBC Papers in Press, December 10, 2001, DOI 10.1074/jbc.M104146200

Shang-Rong Ji, Yi Wu, and Sen-fang Sui‡

From the Department of Biological Sciences and Biotechnology, State-Key Laboratory of Biomembrane, Tsinghua University, Beijing 100084, People's Republic of China

β-Amyloid peptide (Aβ), a normal constituent of neuronal and non-neuronal cells, has been proven to be the major component of extracellular plaque of Alzheimer's disease. Interactions between Aβ and neuronal membranes have been postulated to play an important role in the neuropathology of Alzheimer's disease. Here we show that Aβ is able to insert into lipid bilayer. The membrane insertion ability of Aβ is critically controlled by the ratio of cholesterol to phospholipids. In a low concentration of cholesterol Aβ prefers to stay in membrane surface region mainly in a β-sheet structure. In contrast, as the ratio of cholesterol to phospholipids rises above 30 mol%, Aβ can insert spontaneously into lipid bilayer by its C terminus. During membrane insertion Aβ generates about 60% α-helix and removes almost all β-sheet structure. Fibril formation experiments show that such membrane insertion can reduce fibril formation. Our findings reveal a possible pathway by which Aβ prevents itself from aggregation and fibril formation by membrane insertion.

The formation of extracellular amyloid plaques is one of the characteristics of Alzheimer's disease. The core component of plaque is Aβ,[1] which is the proteolytic product of the larger transmembrane amyloid precursor protein (APP) (1, 2). Aβ contains 39–42 amino acid residues with a molecular mass of approximate 4 kDa. Aβ is an amphiphilic peptide with a hydrophilic N-terminal domain (residues 1–28) and a hydrophobic C-terminal (residues 29–40 (42)), the latter corresponding to a part of the transmembrane domain of APP.

Aβ is a normal constituent of neuronal and non-neuronal cells (3, 4). It can be detected in cerebrospinal fluid at subnanomolar concentrations in normal individuals. Such a concentration of Aβ has its own physiological functions, for example, increasing tyrosine phosphorylation, increasing the activity of phosphoinositol 3-kinase, and inducing the rapid change of cellular calcium and extracellular protein kinase C (5). It was reported that in cultured hippocampal neurons, Aβ at a low concentration (10^{-11}~10^{-10} M) is neurotrophic to undifferentiated, immature hippocampal neurons (6, 7). As a proteolytic fragment of APP, Aβ can be secreted by membrane-anchored APP or by reinternalized APP (8–10). Also, Aβ can be degraded either via LRP-mediated endocytosis into primary neurons and astrocytes (11–15) or via scavenger receptor-mediated uptake of aggregates of Aβ into microglial cells (16). The hydrolytic enzymes in lysosomes then can degrade Aβ. Thus, whether Aβ is the primary effector of the disease is questioned.

Several studies on conformation show that Aβ in the core of amyloid plaques adopts an antiparallel β-sheet (17). So Aβ in the form of β-sheet may be in favor of aggregating into fibril. In addition, *in vitro* studies with cell cultures have demonstrated that fibrillar Aβ is toxic to neurons, but monomeric Aβ is not (18–20). Therefore, the factors inducing Aβ to generate β-sheet may contribute to the pathogenesis of Alzheimer's disease.

The neurotoxicity of Aβ is exhibited in many fields. One of the potential mechanisms for inducing the neurotoxicity of Aβ is direct interaction with the membranes. It has been reported that Aβ is able to form ionic pores (21). Aβ can destroy the structure of brain membranes (22) and may stimulate free radical production by interfering with the regulation of calcium homeostasis and cell enzymatic activity (23). Aβ can also alter the physical-chemical properties of neuronal membranes, including membrane fluidity, membrane lipid dynamics, and the activity of various membrane-bound proteins (24, 25).

In the present work we emphasize how lipid membrane affects the behavior of Aβ. In particular we study the membrane insertion of Aβ(1–40), the major species normally secreted from cells (26), by lipid monolayer and vesicle systems. First, we used the monolayer technique to detect the membrane insertion ability of Aβ. Second, we carried out a combination of MALDI-TOF mass spectrometry (MS) with enzymatic hydrolysis to confirm the membrane insertion of Aβ into phospholipid vesicles. And third, we employed circular dichroism (CD) spectroscopy to study the conformational change of Aβ upon insertion. Finally, electron microscopy work tested that membrane insertion of Aβ could reduce the formation of fibril. Our results show that Aβ(1–40) is able to insert into lipid bilayer and that there is a close correlation between membrane insertion of Aβ and its secondary structure, which is critically dependent upon the ratio of cholesterol to phospholipids. Our findings suggest the possibility that Aβ may prevent itself from aggregating by membrane insertion.

EXPERIMENTAL PROCEDURES

Materials—1,2-Dipalmitoyl-*sn*-glycero-3-phosphocholine (DPPC), 1,2-dimyristoyl-*sn*-glycero-3-phosphocholine (DMPC), and cholesterol were all purchased from Sigma Chemical Co. β-Amyloid peptides Aβ(1–

* The costs of publication of this article were defrayed in part by the payment of page charges. This article must therefore be hereby marked "*advertisement*" in accordance with 18 U.S.C. Section 1734 solely to indicate this fact.

‡ To whom correspondence should be addressed. Tel.: 86-10-6278-4768; Fax: 86-10-6278-4768; E-mail: suisf@mail.tsinghua.edu.cn.

[1] The abbreviations used are: Aβ, β-amyloid peptide; APP, amyloid precursor protein; CCA, α-cyano-4-hydroxycinnamic acid; DPPC, 1,2-dipalmitoyl-*sn*-glycero-3-phosphocholine; 1,2-dimyristoyl-*sn*-glycero-3-phosphocholine; LRP, low density lipoprotein receptor-related protein; MALDI-TOF, matrix-assisted laser desorption/ionization-time-of flight; mN, millinewton; mN/m, millinewton per meter; MS, mass spectrometry; π, monolayer surface pressure; π_i, initial surface pressure; $\Delta\pi$, increase of surface pressure; π_c, critical insertion pressure; PC, phosphatidylcholine; SPM, sphingomyelin.

40) and (1–28) were purchased from AnaSpec Co., whose purity (>95%) was analyzed by high performance liquid chromatography and checked by MALDI-TOF MS. And unless stated, Aβ refers to Aβ(1–40) in the following text. Papain and α-cyano-4-hydroxycinnamic acid (CCA) used in hydrolysis were purchased from Sigma Chemical Co. All other chemicals used were of analytical grade and manufactured in China. Usually the subphase buffer was 50 mM Tris-HCl, pH 7.4, containing 25 mM NaCl.

Monolayer Surface Pressure Measurements—The monolayer surface pressure (π), defined as the change of the surface tension after spreading a monolayer on the water surface, was measured with an NIMA 9000 (England) microbalance. The peptide insertion was determined by a circular Teflon trough with a volume of 4 ml and surface area of 10 cm^2. A filter paper of 1.0-cm width was employed as the Wihelmy plate. The surface pressure measurements were made with the plate in a fixed height position, and the data were automatically collected and recorded by computer.

In general, the experiments were conducted as follows. First, the circular trough was filled with 4 ml of buffer. Then the phospholipid monolayers were prepared by carefully spreading the lipid solution (dissolved in a solvent of chloroform/methanol (3:1, v/v) with a concentration of 1.0 mg/ml) onto the buffer surface. After the surface pressure stabilized at a constant desired value, the initial surface pressure (π_i), Aβ was injected into the subphase through a side sample hole. The pressure change was monitored until the surface pressure increase ($\Delta\pi$) had reached a maximal value, usually within 2 h. The water used was deionized, and the subphase buffer contained 50 mM Tris-HCl, pH 7.4, and 25 mM NaCl. During the measurement, the subphase was stirred continuously with a magnetic bar. The temperature was controlled at 24.0 ± 1.0 °C.

Preparation of Phospholipid Vesicles—Small unilamellar vesicles were prepared as follows. Lipids of the desired composition were mixed in chloroform/methanol (3:1, v/v) and dried under a stream of nitrogen. Residual solvents were removed under high vacuum for 5–7 h. The lipid films were then resuspended and sonicated in the desired buffer to near optical clarity by using a probe sonicator. The metal debris from the titanium tip was eliminated by centrifugation. The concentration of phospholipid was determined by phosphate analysis (27).

Hydrolysis of Aβ—The enzyme used to hydrolyze Aβ was papain, isolated from the latex of *Carica papaya*. Papain consists of a single polypeptide chain with 212 residues, and the molecular mass is about 23 kDa (28). Papain's specific hydrolytic sites are Glu-*X*, Gly-*X*, Tyr-*X*, His-*X*, Lys-*X*, and Arg-*X*. For convenient measurement of MS the enzymatic hydrolysis of Aβ was carried out in low ion strength buffer (10 mM Tris-HAc, pH 7.4) at 37 °C in Eppendorf tubes. In a typical experiment, before hydrolysis, vesicles sonicated in the same buffer reacted with Aβ, and at the same time, Aβ in an identical volume of buffer only (without vesicles) was prepared as a control. The reaction was started by the addition of a certain amount of peptide solution to acquire a 16 (mol/mol) ratio of peptide to enzyme. The final concentration of peptide added was determined by pre-experiments to give the peak of molecular ion. After 40 min of reaction, iodoacetamide was injected to stop the reaction. Then the mixture was used for MALDI-TOF MS analysis.

MALDI-TOF MS—The instrument used here is BIFLEX III MALDI-TOF mass spectrometer made by Bruker Daltonics Co. A pulsed nitrogen laser operating at 337 nm was used to generate the MALDI ions.

The matrix used in these experiments was CCA. CCA was dissolved in a solution of a 1:1 mixture of acetonitrile and water containing 0.1% trifluoroacetic acid for sample preparation. A 0.5-μl aliquot of CCA mixture was added into an Eppendorf tube and then mixed with 0.5 μl of a reaction solution of peptide and papain. The final peptide/matrix mixture in the Eppendorf tube was deposited on a stainless steel probe tip and allowed to dry at room temperature.

Circular Dichroism (CD) Spectroscopy—CD measurements were carried out on a Jasco J-715 spectropolarimeter. Samples were scanned at least 10 times at the rate of 200 nm/min with a 0.5 nm step, 1 nm bandwidth, and then averaged. The path length of the quartz cell was 2 mm. In the experiments, a blank run made with the vesicles or buffer alone was carefully subtracted from the experimental spectra for correction. The 200–250 nm spectra were used for analysis and calculation because in this wavelength range, the vesicle scattering had little effect on the CD spectra. All spectra were smoothed and converted to the mean residue ellipticity, [θ] in deg*cm^2/dmol, by using a mean residue molecular mass of 110; the secondary structure of the peptide was estimated from spectral simulations based on reference CD spectra of Yang *et al*. (29).

In a general experiment, a desired amount of vesicle solution, determined by a lipid:protein ratio of 100, was added to an Eppendorf tube, and then 1 mg/ml Aβ was injected to acquire a final concentration of 0.1 mg/ml. After incubation for 90 min (providing enough time for the interaction between Aβ and vesicles), the mixture was measured by the spectropolarimeter.

Electron Microscopy—For the vesicle-containing the sample preparation, vesicle solution was first added into an Eppendorf tube, and then a certain amount of protein solution was injected to reach a final protein concentration of 0.2 mg/ml. After storage at 37 °C for 2 days the vesicle suspensions were applied to carbon-coated copper grids, dried, negatively stained with 2% (w/v) uranyl acetate, and visualized in a Philips CM120 transmission electron microscopy operated at 120 kV. As a control the same procedure was performed for the sample containing only peptide without vesicles.

RESULTS

Monolayer Experiments—In the experiments we have applied a model that assumes that the surface pressure will increase only when the protein inserts into the monolayer, and the surface pressure, as reported earlier (30), does not increase if the protein only interacts with the phospholipid head group. Thus, when peptide molecules are injected into the subphase, the corresponding change in surface pressure ($\Delta\pi$) can be interpreted as the result of the peptide inserting into the lipid monolayer. $\Delta\pi$ can be obtained as a function of various π_i for each sample, and then the plot of $\Delta\pi$ *versus* π_i yields a straight line with negative slope which intersects the abscissa at a limiting surface pressure. The limiting surface pressure is defined as the critical insertion pressure (π_c) of Aβ for the corresponding lipid monolayer, which is used as a quantitative measure to evaluate the insertion ability of the peptide to the phospholipid monolayer.

To acquire appropriate conditions of the experiments, first the surface activity of Aβ was detected by measuring the self-penetration of Aβ into the air-water interface without spread lipid monolayer. The peptide solution was injected into the subphase to a final concentration of 200, 400, 500, 600, and 800 nM, and the surface pressure was then measured and plotted *versus* the reaction time. The results (data not shown) show that Aβ could significantly increase the surface pressure, which indicates its strong surface activity. The maximum $\Delta\pi$ induced by the self-penetration of Aβ was found to be 13.7 mN/m, and the minimum concentration of Aβ to reach such a maximum was 500 nM. Thus, we kept π_i of the lipid monolayers spread onto the subphase surface at or above 15.0 mN/m and the concentration of Aβ injected into the subphase at 500 nM in the following experiments.

To measure the ability of Aβ to insert into phospholipid monolayers at the air-water interface, samples of different phospholipids were used. Fig. 1*A* shows the plots of $\Delta\pi$ *versus* π_i of Aβ for pure DPPC monolayer and for its mixtures with different molar fraction of cholesterol. From the plots of Fig. 1*A* the values of π_c are obtained to be 26.6 mN/m for DPPC, and 26.2, 26.2, 32.1, 34.1, and 33.8 mN/m for DPPC containing 20, 25, 33, 56, and 74 mol% cholesterol, respectively. Fig. 1*B* shows the correlation between π_c and mol content of cholesterol. Clearly, there is a sharp increase in π_c as the content of cholesterol rises above 30 mol%. The same insertion experiments of Aβ were performed also for DMPC and cholesterol mixtures (data not shown). We found that the value of π_c for pure DMPC was ~25 mN/m and for 33% cholesterol-containing DMPC ~31 mN/m. DMPC exhibits a cholesterol effect similar to that of DPPC. These results indicate that cholesterol can strongly influence the insertion ability of Aβ into PC monolayers.

Further experiments, as shown in Fig. 2, were performed for PC monolayers containing a certain amount of sphingomyelin (SPM) and cerebroside, imitating the content in brain membrane. From the $\Delta\pi \sim \pi_i$ curves of Fig. 2, it can be seen that only the addition of SPM or cerebroside has little influence on the insertion ability of Aβ. In the presence of 33% cholesterol,

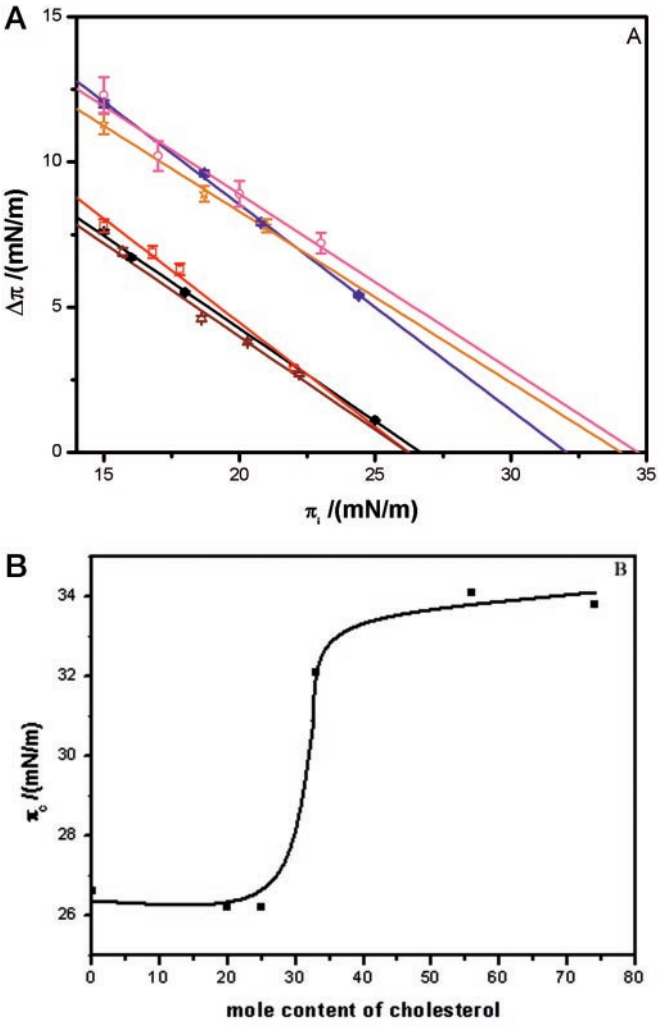

FIG. 1. **$\Delta\pi\sim\pi_i$ curves of Aβ interacting with DPPC monolayers containing different contents of cholesterol (*panel A*) and the correlation between the critical insertion pressure π_c and the molar fraction of cholesterol (*panel B*), where the phospholipids are DPPC (●), DPPC and 20% cholesterol (□), DPPC and 25% cholesterol (△), DPPC and 33% cholesterol (♦), DPPC and 56% cholesterol (☆), and DPPC and 74% cholesterol (○).** The concentration of Aβ is 500 nM, the buffer is 50 mM Tris-HCl and 25 mM NaCl at pH 7.4. Each point in the figure is the average value of three independent experiments.

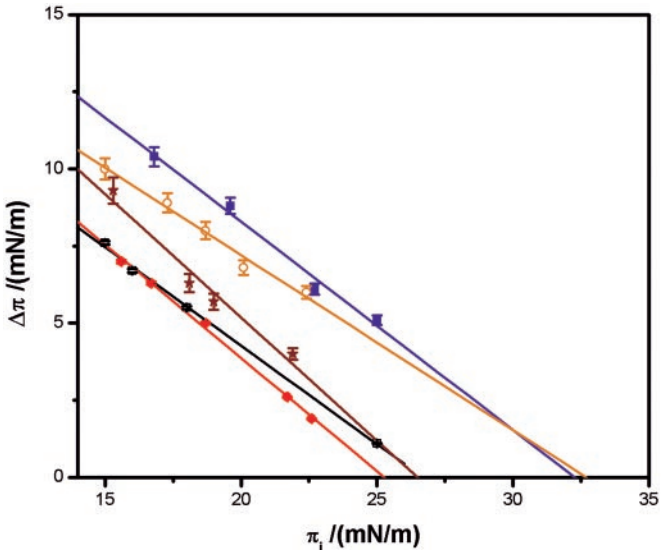

FIG. 2. **$\Delta\pi\sim\pi_i$ curves of Aβ interacting with monolayer mixtures of DPPC and SPM (20 mol%) and DPPC and cerebroside (2.3 mol%) with or without 33 mol% cholesterol, where the monolayer mixtures are DPPC (□), DPPC and SPM (●), DPPC and cerebroside (⋆), DPPC, cerebroside, and cholesterol (■), and DPPC, SPM, and cholesterol (○).** The experimental conditions are as in Fig. 1.

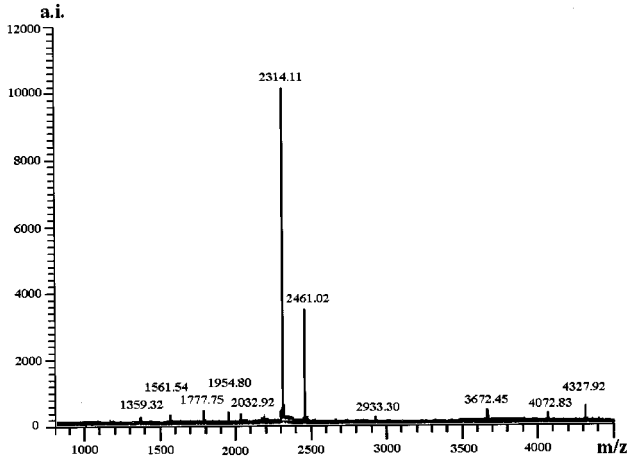

FIG. 3. **MS spectrum obtained for the hydrolysis fragments of free Aβ.** The enzyme used to hydrolyze Aβ is papain, and the buffer was 10 mM Tris-HAc at pH 7.4 only for the convenience measured by mass spectrometry. The temperature was 37 °C. The identification of the peaks of MS is summarized in Table I.

however, for both mixtures, PC/SPM and PC/cerebroside, the π_c is obviously shifted to higher surface pressure, 32–33 mN/m. Such behavior provides evidence that it is cholesterol that contributes to the most increase of π_c. In addition, the correlation between π_c and mol fraction of cholesterol in PC/SPM mixtures was also measured (data not shown). The result showed a behavior similar to that exhibited in Fig. 1*B*, indicating again that the insertion ability of Aβ has a sharp increase when the content of cholesterol higher than 30 mol%.

The above results indicate that the insertion ability of Aβ(1–40) is critically dependent upon the ratio of cholesterol to phospholipids. It has been established that the biological membrane pressure is 31–34 mN/m (31). The packing density of lipid monolayer with a surface pressure in this region can be assumed to be comparable with that of lipid bilayer (32, 33). Therefore, Aβ(1–40) should be able to insert into the lipid bilayer in which the content of cholesterol is above 30%.

The same insertion experiments were performed for Aβ(1–28), and we found that Aβ(1–28) had no surface activity and thus could not induce the increase of surface pressure for different phospholipid monolayers (data not shown). This may be the result of the hydrophilic property of Aβ(1–28) which prevents the peptide from inserting into the monolayers.

MALDI-TOF MS—To confirm whether Aβ(1–40) could insert into lipid bilayer, papain as a protease was used to hydrolyze Aβ after it reacted with lipid vesicles, and the hydrolysis products were analyzed by MALDI-TOF MS. The MS spectrum, which was used to determine the hydrolysis fragments (indicated by *m/z*), obtained for free Aβ (without vesicles), was analyzed at first. The spectrum is shown in Fig. 3, and the peaks identified by MS are summarized in Table I. From Table I we can see that papain treatments only result in a partial hydrolysis of potential sites of cleavage, which may be the result of some second structure of Aβ preventing more cleavage. In the spectra only the peaks with an *m/z* value higher than 1,000 are exhibited because the substances in matrix (such as CCA and its contaminants giving peaks at low *m/z*) can cause interference at low *m/z*. Some non-papain cleavage

TABLE I
Results of hydrolysis of Aβ by papain

The hydrolysis lasted for 40 min after the addition of papain into Aβ solution, and then iodoacetamide was injected to end the reaction. The mixture was detected by MS after mixing with the matrix-CCA.

No.	Cleavage sites	Fragment	M + H$^+$ (*m*/*z*)	
			Calculated	By MALDI
1	Arg^5-His^6, Gly^{25}-Ser^{26}	^{6}HDSGYEVHHQKLVFFAEDVG^{25}	2,314.08	2,314.11
2	Arg^5-His^6, Gly^{25}-Ser^{26}	^{6}HDSGYEVHHQKLVFFAEDVG^{25}	2,336.08+(Na)	2,336.01
3	Gly^{33}-Leu^{34}	^{1}DAEFRHDSGYEVHHQKLVFFAEDVGSNKGAIIG^{33}	3,672.78	3,672.45
4	Gly^{37}-Gly^{38}	^{1}DAEFRHDSGYEVHHQKLVFFAEDVGSNKGAIIGLMVG^{37}	4,072.99	4,072.83
5	Lys^{16}-Leu^{17}	^{1}DAEFRHDSGYEVHHQK^{16}	1,954.87	1,954.80
6		^{1}DAEFRHDSGYEVHHQKLVF^{19}	2,314.09	2,314.11
7		^{1}DAEFRHDSGYEVHHQKLVF^{19}	2,336.09 (+Na)	2,336.01
8		^{20}FAEDVGSNKGAIIGLMVGGVV^{40}	2,033.07	2,032.92
9		^{20}FAEDVGSNKGAIIGLMVGGVV^{40}	2,055.07 (+Na)	2,055.08
10		^{1}DAEFRHDSGYEVHHQKLVFF^{20}	2,461.16	2,461.02
11		^{1}DAEFRHDSGYEVHHQKLVFF^{20}	2,483.16 (+Na)	2,483.13
12		^{21}AEDVGSNKGAIIGLMVGGVV^{40}	1,885.99	1,885.83
13	His^{13}-His^{14}	^{1}DAEFRHDSGYEVH^{13}	1,561.66	1,561.54
14	His^6-Asp^7, Gly^{25}-Ser^{26}	^{7}DSGYEVHHQKLVFFAEDVG^{25}	2,177.02	2,177.00
15	His^6-Asp^7, Gly^{25}-Ser^{26}	^{7}DSGYEVHHQKLVFFAEDVG^{25}	2,199.02 (+Na)	2,199.08
16	Gly^{37}-Gly^{38}	^{20}FAEDVGSNKGAIIGLMVG^{37}	1,777.91	1,777.75
17	Gly^{37}-Gly^{38}	^{20}FAEDVGSNKGAIIGLMVG^{37}	1,799.91 (+Na)	1,799.89
18	Tyr^{10}-Glu^{11}, Gly^{25}-Ser^{26}	^{11}EVHHQKLVFFAEDVG^{25}	1,777.88 (+Na)	1,777.75
19	Arg^5-His^6, Lys^{16}-Leu^{17}	^{6}HDSGYEVHHQK^{16}	1,358.60 (+Na)	1,359.32
20	Tyr^{10}-Glu^{11}, Gly^{37}-Gly^{38}	^{11}EVHHQKLVFFAEDVGSNKGAIIGLMVG^{37}	2,933.51 (+Na)[a]	2,933.30

[a] Met is oxidized.

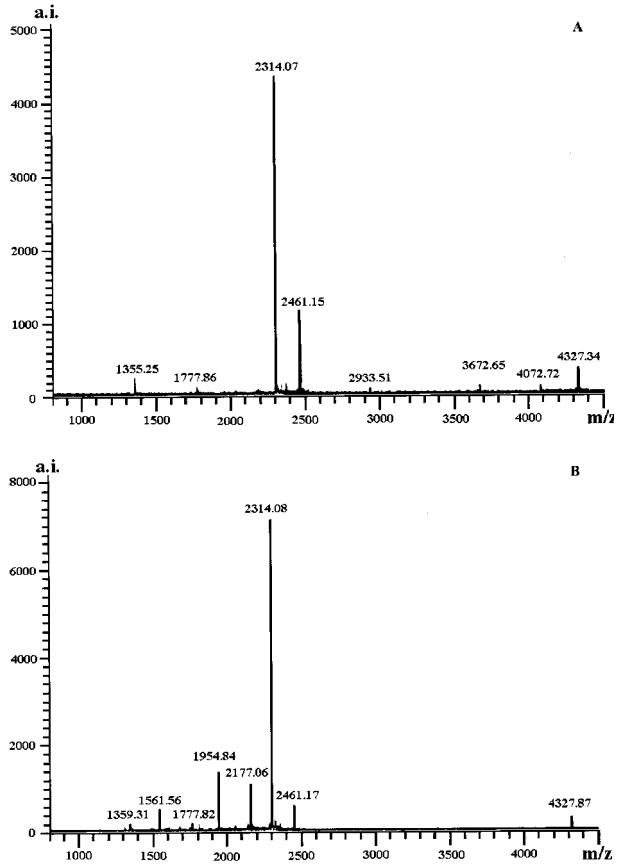

FIG. 4. **MS spectra obtained for the hydrolysis fragments of Aβ after reacting with pure DMPC vesicles (*panel A*) and with 33% cholesterol-containing DMPC vesicles (*panel B*).** The measurement conditions are as in Fig. 3.

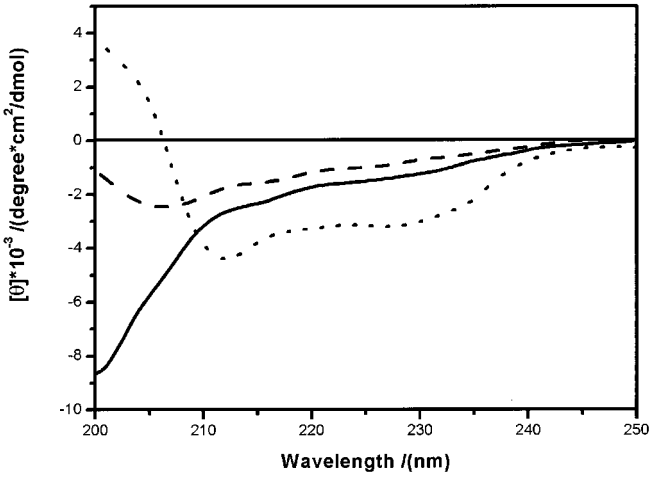

FIG. 5. **CD spectra of Aβ in pure buffer (——) and after reacting with vesicles of pure DMPC (– – –) and 33% cholesterol-containing DMPC (·····), respectively.** The buffer used here contains 50 mM Tris-HCl and 25 mM NaCl at pH 7.4.

fragments in Table I may be the result of the broken peptide because some peptide bonds may be readily broken during flying in the MS experiments.

The MALDI-TOF MS spectra of the hydrolysis products for Aβ reacting with DMPC and 33% cholesterol-containing DMPC vesicles are shown in Fig. 4. For reaction with DMPC vesicles the MS peaks are nearly identical with that of free Aβ. This result provides evidence that papain can approach nearly all cleavage sites as for free Aβ, indicating that Aβ does not insert into such lipid vesicles. In contrast, after reaction with 33% cholesterol-containing DMPC vesicles, as shown in Fig. 4*B*, the characteristic peaks of the MALDI-TOF MS spectrum of Aβ have a considerable change. Several fragments that could be obtained from free Aβ have disappeared here, such as the peaks of *m*/*z* 2,932, 3,672, and 4,072. By comparing the difference in the spectra among them in Fig. 4, we can find that the inaccessible cleavage sites are Gly^{33}-Leu^{34} and Gly^{37}-Gly^{38}. Both sites are located in the C-terminal region of Aβ. This phenomenon can be explained as their locus in the membrane insertion part of Aβ, which protects them from being cleaved by papain. These results lead to the conclusion that Aβ indeed inserts into the rich cholesterol-containing vesicles by its C-terminal domain.

The same experiments were performed also for Aβ(1–28), and no such effect was found (data not shown). This may be evidence that no membrane insertion occurs for Aβ(1–28).

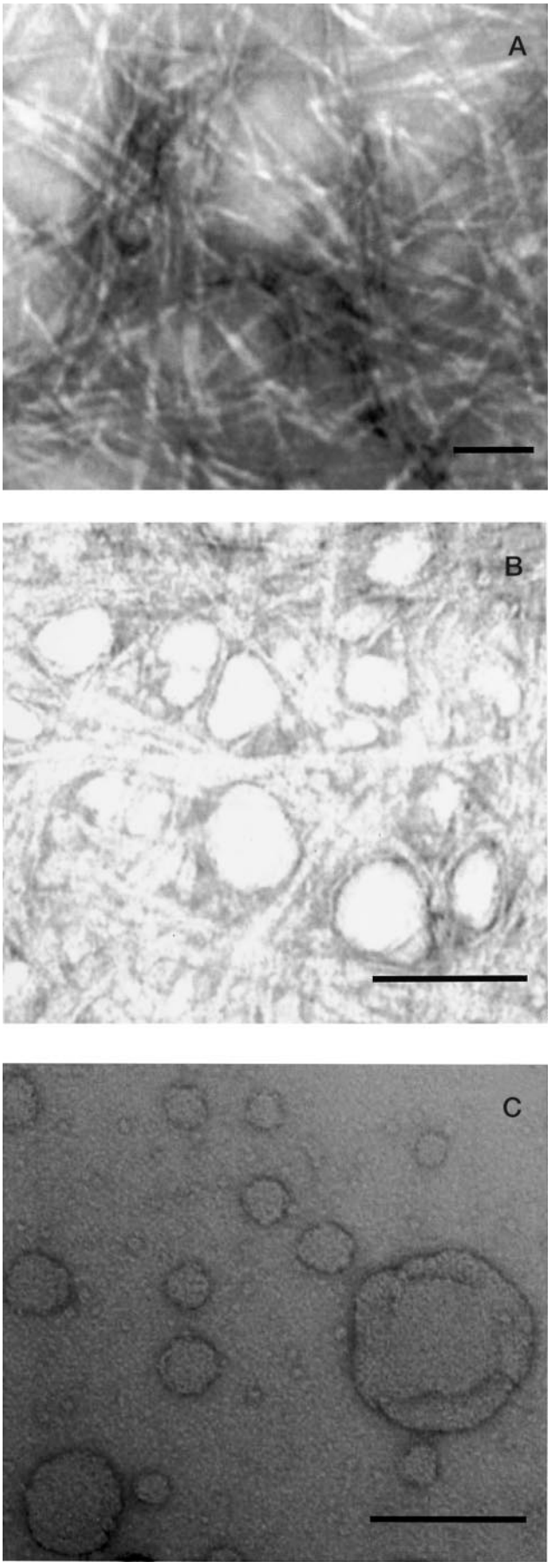

FIG. 6. **Electron micrographs of negative-stained preparations of Aβ(1–40) in the presence and absence of vesicles.** Preparations of 0.2 mg/ml Aβ(1–40) in buffer alone (*panel A*), in the presence of DMPC vesicles (*panel B*), and in the presence of 33% cholesterol-containing DMPC vesicles (*panel C*) were incubated in 50 mM Tris-HCl buffer for 2 days at 37 °C. The *bar* in the figure represents 100 nm.

Circular Dichroism—Whether there is a conformational change of Aβ during membrane insertion is a crucial question because the conformation of Aβ may be related to its aggregation (17). Here CD spectroscopy was employed to measure the secondary structure change. Before the CD measurement a pre-experiment was performed to determine the critical molar ratio for Aβ binding, which is defined as the minimal ratio of lipid to Aβ for maximal binding of Aβ to lipid vesicles. In the present case the critical molar ratio of lipid to Aβ of about 50 was obtained. Thus in the following measurements we choose 100 as the actual lipid:Aβ ratio to assure enough lipid.

Fig. 5 shows three CD spectra acquired from lipid-free Aβ, Aβ reacted with DMPC, and with 33% cholesterol-containing DMPC vesicles. The CD spectrum of lipid-free Aβ is typical of a peptide containing significant random-coil content. The computer fit results show that lipid-free Aβ consists of 48.9% random-coil, 23.5% β-sheet, and 1.7% α-helix. The results are consistent with the reports of Terzi *et al.* (1, 34). The addition of DMPC and 33% cholesterol-containing DMPC vesicles leads to a remarkable alteration in the CD curves as also shown in Fig. 5, indicating that Aβ undergoes a significant conformational change. According to the computer fit results one can see that in the case of the addition of DMPC vesicles, both contents of β-sheet and α-helix have about a 7% increase, *i.e.* the β-sheet increased to 31.2% and α-helix to 9.5%. In contrast, when 33% cholesterol-containing DMPC vesicle was added, the structure of Aβ altered drastically. The β-sheet structure decreased to zero, and the α-helix increased remarkably to 58.8%. Such results indicate that membrane insertion of Aβ eliminates its β-sheet structure and induces its α-helices.

In addition, the effect of pH on Aβ secondary structure was tested by means of CD. First, Aβ in solution with different pH was measured, and the result (data not shown) indicated that pH had a certain influence on the Aβ secondary structure, which was similar to that of McLaurin and Chakrabartty's work (35). Then the conformations of Aβ after reacting with cholesterol-rich vesicles at different pH were measured (data not shown). The results showed that little influence could be observed, indicating that the final state of membrane inserted Aβ was not sensitive to pH, which is not the case of Aβ in solution.

The above measurements were performed also for Aβ(1–28), and the results (data not shown) show that there is almost no conformational change induced by lipid vesicles, which again is an indication of the hydrophilic property of Aβ(1–28).

Electron Microscopy—The effect of phospholipid vesicles on the formation of Aβ(1–40) fibrils was examined by electron microscopy. As shown in Fig. 6*A*, Aβ(1–40), dissolved in pH 7.4 Tris-HCl buffer, with a concentration of 0.2 mg/ml, could assemble into filaments *in vitro*. But the addition of vesicles produced significantly different results in the same peptide concentration: filaments could be still observed in DMPC vesicles (Fig. 6*B*), and almost no filaments were observed in 33% cholesterol-containing DMPC vesicles (Fig. 6*C*).

DISCUSSION

Cholesterol is an integral component of all eukaryotic cell membranes and is essential for normal cellular functions (36, 37). Cholesterol is not distributed uniformly within the cell. The plasma membrane contains the highest levels of cholesterol (nearly 90% of total cellular cholesterol) (38), and it was demonstrated that the cholesterol:phospholipid ratio of the plasma membranes is about 0.52~0.70 (mol/mol) (39–41).

Even in a certain membrane, cholesterol is distributed asymmetrically enriched in cytofacial leaflet (42, 43). It was noticed that cholesterol in the cytofacial leaflet of brain synaptic plasma membrane is about 87% of total plasma membrane cholesterol when young, but the distribution of cholesterol tends to be homogeneous in the cytofacial and exofacial leaflet during the aging process (44); cholesterol of plasma membranes in the nervous system also increases with age (45). The cholesterol ratio of brain plasma membrane, one can estimate, is at least 30 mol% when aged. Thus, the currently used model membrane system simulates the normal aged physiological condition to a certain extent.

Two model membrane systems were employed in the current work, *i.e.* monolayer and vesicle (closed bilayer). The lipid monolayer is a unique system to distinguish the functional role of a particular component in the membrane mixtures. According to the monolayer results obtained from Figs. 1 and 2, it is cholesterol, when at high but physiologically reasonable level, which could obviously enhance the insertion ability of Aβ, whereas other brain membrane components such as SPM and cerebroside could not. A big inspiration drawn from the monolayer experiments is that the insertion ability of Aβ can be high enough, in the present case $\pi_c > 31$ mN/m, for it to insert into lipid bilayer. This result has been proved by the MS analysis of hydrolytic products with vesicle system. The MS measurements provided direct evidence (as shown in Fig. 4) that Aβ can really insert into the lipid vesicles containing rich cholesterol, but it cannot without cholesterol. The MS measurements also determined that the membrane insertion of Aβ is by its C terminus. This is quite reasonable because hydrophobic domain is located there.

The membrane-induced conformational change is investigated in the present work by a CD technique with the vesicle system. This should be a very important problem because the behavior of membrane insertion of Aβ may be related to its neurotoxicity by its conformational change. Several laboratories have reported their CD work on Aβ. Different experimental conditions may induce different Aβ conformations: (i) the α-helix in trifluoroethanol, SDS micelles, or induced by ganglioside-containing vesicles (34, 35, 46–49), and also in our experiments when we used ethanol-water system to simulate the membrane condition, and the CD results indicate that the α-helix increases along with an increase of the ethanol content (data not shown), which coincides with the previous reports very well; (ii) essentially random-coil structures with β-turns in aqueous solution at low peptide concentrations; and (iii) β-structured aggregates in solution or in contact with lipid membranes (2, 34). So far to our knowledge, systems containing cholesterol, which assuredly is the common component of membranes, are not employed yet in these published papers.

From our CD results shown in Fig. 5, one can see that Aβ in aqueous solution adopts a conformation mainly in random-coil; whereas when reacted with DMPC vesicles it contains more β-sheet, and then when reacted with cholesterol-containing vesicles it becomes mainly in α-helix. One interesting phenomenon is that a certain conformational change occurs even when Aβ reacts with DMPC vesicles. From the monolayer surface pressure measurements, as mentioned before, the π_c for the PC monolayer is around 26 mN/m, suggesting that Aβ cannot insert into this kind of lipid bilayer. The MS analysis of hydrolytic products supported the monolayer results because papain could approach nearly all of the cleavage sites of Aβ after reacted with DMPC. On the other hand, however, the surface pressure measurement on self-penetration of Aβ shows that Aβ is a peptide with a strong surface activity. This quality of Aβ makes it prefer to stay in an amphiphilic environment, *i.e.* membrane surface region. The physical chemistry property in the membrane surface region is different from that in the inner bilayer and in the bulk, which has been widely reported. That such a difference may induce protein conformational change has also been noticed (50). Therefore, although Aβ cannot insert into PC bilayer, a certain conformation change may also happen when it reaches the membrane surface region. This is possibly the case when Aβ reacts with DMPC vesicles. A quite important point is that under such case Aβ adopts considerable structure in β-sheet, suggesting that the aggregation of Aβ may occur around the surface region of membranes because β-sheet may be a factor inducing Aβ aggregation. This coincides with the previous direct observation by using confocal laser scanning microscope and transmission electron microscopy (2, 51–53).

Another crucial point we obtained is that Aβ adopts mainly an α-helix after reacting with rich cholesterol-containing PC vesicles. This effect could be beneficial in reducing the formation of aggregation by depressing the β-sheet conformation, suggesting that a possible pathway of Aβ aggregation which ultimately induces the formation of plaques may be prevented by its membrane insertion. The electron micrographs shown in Fig. 6 provid a direct test performed *in vitro* to support this hypothesis: the addition of rich cholesterol-containing vesicles could effectively depress the formation of Aβ(1–40) fibrils, whereas pure DMPC could not.

According to the above results we know the forms of Aβ: (i) existing in the aqueous solution and adopting a random-coil conformation; (ii) existing in the surface region of vesicles and adopting a conformation containing more β-sheet, such as interaction with DMPC vesicles; (iii) inserting into rich cholesterol-containing membranes and adopting an α-helix conformation. Altogether, our data show that the existence forms of Aβ obviously depended on the ratio of cholesterol to phospholipid of membranes, which reflects the fact that membrane cholesterol distribution could be an important event in the Aβ-related disease.

Aβ generated to perform its physiological function can be degraded through endocytosis, such as via LRP or via a scavenger receptor. But when aged, one of the important changes for Aβ metabolism is that LRP will reduce ~45% (54). The decrease of LRP will partly block the degradation pathway of Aβ, which would increase the extracellular content of Aβ. If the content of Aβ cannot be reduced, it would aggregate and form plaques. The increase of cholesterol, also a change with aging, may be a compensatory factor reducing extracellular Aβ by membrane insertion (according to our results). In the case of Alzheimer's disease subjects, however, a significant difference is present: brain membranes isolated from them show dramatic decreases in membrane cholesterol content (the ratio of cholesterol to phospholipids decreases about 30%) (55, 56). Under such conditions, Aβ may be not able to insert into membrane to avoid aggregation.

REFERENCES

1. Terzi, E., Hölzemann, G., and Seelig, J. (1995) *J. Mol. Biol.* **252,** 633–642
2. McLaurin, J., Franklin, T., Chakrabartty, A., and Fraser, P. E. (1998) *J. Mol. Biol.* **276,** 183–194
3. Esch, F. S., Keim, P. S., Beattie, E. C., Blacher, R. W., Culwell, A. R., Oltesdorf, T., McClure, D., and Word, P. J. (1990) *Science* **248,** 1122–1128
4. Haass, C., Schlossmacher, M. G., Hung, A. Y., Vigo-Pelfrey, C., Mellon, A., Ostaszewski, B. L., Lieberburg, I., Koo, E. H., Schenk, D., Teplow, D. B., and Selkoe, D. J. (1992) *Nature* **359,** 322–325
5. Mills, J., and Reiner, P. B. (1999) *J. Neurochem.* **72,** 443–460
6. Seubert, P., Vigo-Pelfrey, C., Esch, F., Lee, M., Dovey, H., Davis, D., Sinha, S., Schlossmacher, M., Whaley, J., Swindlehurst, C., McCormack, R., Wolfert, R., Selkoe, D., Lieberburg, I., and Schenk, D. (1992) *Nature* **359,** 325–327
7. Shoji, M., Golde, T. E., Ghiso, J., Cheung, T. T., Estus, S., Shaffer, L. M., Cai, X. D., McKay, D. M., Tintner, R., Frangione, B., and Younkin, S. G. (1992) *Science* **258,** 126–129
8. Haass, C., Koo, E. H., Mellon, A., Hung, A. Y., and Selkoe, D. J. (1992) *Nature* **357,** 500–502

9. Koo, E. H., and Squazzo, S. L. (1994) *J. Biol. Chem.* **269,** 17386–17389
10. Koo, E. H., Squazzo, S. L., Selkoe, D. J., and Koo, C. H. (1996) *J. Cell Sci.* **109,** 991–998
11. Blacker, D., Wilcow, M. A., Laird, N. M., Rodes, L., Horvath, S. M., Go, R. C. P., Perry, R., Watson, B., Jr., Bassett, S. S., McInnis, M. G., Albert, M. S., Hyman, B. T., and Tanzi, R. E (1998) *Nat. Genet.* **19,** 357–360
12. Narita, M., Holtzman, D. M., Schwartz, A. L., and Bu, G. J. (1997) *J. Neurochem.* **69,** 1904–1911
13. Hughes, S. R., Khorkova, O., Goyal, S., Knaeblein, J., Heroux, J., Riedel, N. G., and Sahsrabudhe, S. (1998) *Proc. Natl. Acad. Sci. U. S. A.* **95,** 3275–3280
14. Kovacs, D. M. (2000) *Exp. Gerontol.* **35,** 473–479
15. Janciauskiene, S., Wright, H. T., and Linidgren, S. (1999) *Neuropeptides* **33,** 510–516
16. Paresce, D. M., Ghosh, R. N., and Maxfield, F. R. (1996) *Neuron* **17,** 553–565
17. Inouye, H., Fraser, P. E., and Kirschner, D. A. (1993) *Biophys. J.* **64,** 502–519
18. Pike, C. J., Burdick, D., Walencewicz, A. J., Glabe, C. G., and Cotman, C. W. (1993) *J. Neurosci.* **13,** 1676–1687
19. Simmons, L. K., May, P. C., Tomaselli, K. J., Rydel, R. E., Fuson, K. S., Brigham, E. F., Wright, S., Lieberburg, I., Becker, G. W., and Brems, D. N. (1993) *Mol. Pharmacol.* **45,** 373–379
20. Lorenzo, A., and Yankner, B. (1994) *Proc. Natl. Acad. Sci. U. S. A.* **91,** 12243–12247
21. Arispe, N., Pollard, H. B., and Rojas, E. (1993) *Proc. Natl. Acad. Sci. U. S. A.* **90,** 10573–10577
22. Eckert, G. P., Cairns, N. J., Maras, A., Gattaz, W. F., and Muller, W. E. (2000) *Dementia Geriatric Cognitive Dis.* **11,** 181–186
23. Waiter, M. F., Mason, P. E., and Mason, R. P. (1997) *Biochem. Biophys. Res. Commun.* **233,** 760–764
24. Martinez-Senac, M. M., Villalaín, J., and Gómez-Fernández, J. C. (1999) *Eur. J. Biochem.* **265,** 744–753
25. Mason, R. P., Estermyer, J. D., Kelly, J. F., and Mason, P. E. (1996) *Biochem. Biophys. Res. Commun.* **222,** 78–82
26. Roher, A. E., Clarke, S., Wood, A. S., Cotter, R. J., Gowing, E., and Ball, M. J. (1993) *Proc. Natl. Acad. Sci. U. S. A.* **90,** 10836–10840
27. Ames, B. N. (1966) *Methods Enzymol.* **8,** 115–118
28. Zhuang, P., and Butterfield, D. A. (1991) *Biophys. J.* **60,** 623–628
29. Yang, J. T., Wu, C. S. C., and Martinez, H. M. (1986) *Methods Enzymol.* **130,** 208–269
30. Demel, R. A., London, Y., and Geurts Van Kessel, W. S. (1973) *Biochim. Biophys. Acta* **311,** 507–519
31. Demel, R. A., Geurts Van Kessel, W. S., Zwaal, R. F., Roelofsen, B., and van Deenen, L. L. (1975) *Bichim. Biophys. Acta* **406,** 97–107
32. Seelig, A. (1987) *Biochim. Biophys. Acta* **899,** 196–204
33. Smaby, J. M., Momsen, M., Kulkarni, V. S., and Brown, R. E. (1996) *Biochemistry* **35,** 5696–5704
34. Terzi, E., Hölzemann, G., and Seelig, J. (1997) *Biochemistry* **36,** 14845–14852
35. McLaurin, J., and Chakrabartty, A. (1996) *J. Biol. Chem.* **271,** 26482–26489
36. Howland, D. S., Trusko, S. P., Savager, M. J., Reaume, A. G., Lang, D. M., Hirsch, J. D., Maeda, N., Siman, R., Greenberg, B. D., Scott, R. W., and Flood, D. G. (1998) *J. Biol. Chem.* **273,** 16576–16582
37. Brown, M. S., and Goldstein, J. L. (1997) *Cell* **89,** 331–340
38. Yeagle, P. L. (1985) *Biochim. Biophys. Acta* **822,** 267–287
39. Chakravarthy, B. R., Spence, M. W., Clarke, J. T. R., and Cook, H. W. (1985) *Biochim. Biophys. Acta* **812,** 223–233
40. Depauw, H., Wolf, M., Dessel, G., Hilderson, H. J., Lagrou, A., and Dierick, W. (1985) *Biochim. Biophys. Acta* **814,** 57–67
41. Lange, Y., Swaisgood, M. H., Ramos, B. V., and Steck, T. L. (1989) *J. Biol. Chem.* **264,** 3786–3793
42. Schroeder, F., Jefferson, J. R., Kier, A. B., Knittel, J., Scallen, T. J., Wood, W. G., and Hapala, I. (1991) *Proc. Soc. Exp. Biol. Med.* **196,** 235–252
43. Schroeder, F., Woodford, J. K., Kavecansky, J., Wood, W. G., and Joiner, C. (1995) *Mol. Membr. Biol.* **12,** 113–119
44. Igbavboa, U., Avdulov, N. A., Schroeder, F., and Wood, W. G. (1996) *J. Neurochem.* **66,** 1717–1725
45. Shinitzky, M. (ed) (1993) *Biomembranes*: *Structural and Functional Aspects*, pp. 1–82, John Wiley & Sons, New York
46. Barrow, C. J., and Zagorski, M. G. (1991) *Science* **253,** 180–182
47. Sticht, H., Bayer, P., Willbold, D., Dames, S., Hillbich, C., Beyreuther, K., Frank, R. W., and Rösch, P. (1995) *Eur. J. Biochem.* **233,** 293–298
48. Coles, M., Bicknell, W., Watson, A. A., Fairlie, D. P., and Creik, D. J. (1998) *Biochemistry* **37,** 11064–11077
49. McLaurin, J., Franklin, T., Fraser, P. E., and Chakrabartty, A. (1998) *J. Biol. Chem.* **273,** 4506–4515
50. Sui, S. F. (2000) *Adv. Colloid Interface Sci.* **85,** 257–267
51. Choo-Smith, L., Garzon-Rodriguez, W., Glabe, C. G., and Surewicz, W. K. (1997) *J. Biol. Chem.* **272,** 22987–22990
52. Mattson, M. P., Barger, S. W., Cheng, B., Lieberburg, I., Smith-Swintosky, V. L., and Rydel, R. E. (1993) *Trends Neurosci.* **16,** 409–414
53. Avdulov, N. A., Chochina, S. V., Igbavboa, U., Warden, C. S., Vassiliev, A. V., and Wood, W. G. (1997) *J. Neurochem.* **69,** 1746–1752
54. Christie, R. H., Ghung, H., Rebeck, G. W., Strickland, D., and Bradley, T. (1996) *J. Neuropathol. Exp. Neurol.* **55,** 491–498
55. Mason, R. P., Shoemaker, W. J., Shajenko, L., Chambers, T. E., and Herbette, L. G. (1992) *Neurobiol. Aging* **13,** 413–419
56. Roth, G. S., Joseph, J. A., and Mason, R. P. (1995) *Trends Neurosci.* **18,** 203–206